# Characterization of microwave effects on metal-oxide materials: Zinc oxide and titanium dioxide

Satoshi Horikoshi [a,b,*], Akihiro Matsubara [c], Sadatsugu Takayama [d], Motoyasu Sato [d], Futoshi Sakai [b], Masatsugu Kajitani [b], Masahiko Abe [a], Nick Serpone [e,**]

[a] Research Institute for Science and Technology, Tokyo University of Science, 2641 Yamazaki, Noda, Chiba 278-8510, Japan
[b] Department of Materials and Life Sciences, Faculty of Science and Technology, Sophia University, 7-1 Kioicho, Chiyoda, Tokyo 102-8554, Japan
[c] Center for Advanced Metrology, Chubu University, 1200, Matsumoto, Kasugai, Aichi 487-8501, Japan
[d] Coordination Research Center, National Institute for Fusion Science, 322-6 Oroshi, Toki, Gifu 509-5292, Japan
[e] Gruppo Fotochimico, Dipartimento di Chimica Organica, Universita di Pavia, Via Taramelli 10, Pavia 27100, Italy

## ARTICLE INFO

## ABSTRACT

The microwave specific effect(s) that can impact a microwave-assisted and photo-assisted reaction occurring on the surface of ZnO or TiO$_2$ (P-25) particles was (were) examined by comparing the process occurring under rich magnetic field conditions and under magnetic/electric field conditions. The features of the photo-assisted process in the presence of microwaves rich in a magnetic field ($\mathbf{H}$) and an electric field ($\mathbf{E}$) are described on the basis of (i) the degradation dynamics of 4-chlorophenol (4-CP) at ambient temperatures, (ii) the number of $^\bullet$OH radicals produced, and (iii) the dielectric properties of the metal oxides (in pellet form). For ZnO, the photoactivity is enhanced by a microwave specific non-thermal (i.e. non-caloric) effect originating from the microwaves' magnetic field, but decreased by the thermal (i.e. caloric) factor originating from the microwaves' electric field. Contrary to ZnO, the photoactivity of TiO$_2$ (P-25) was enhanced by the synergistic effect between the magnetic and electric fields of the microwave radiation. Photocorrosion of ZnO in the aqueous dispersions was negligibly small (less than 0.05%) under UV, MW-$\mathbf{EH}$, and UV/MW-$\mathbf{EH}$ irradiation conditions.

© 2009 Elsevier B.V. All rights reserved.

## 1. Introduction

Reactions of organic compounds taking place on a ZnO powdered specimen, often used as a semiconductor photocatalyst, have been examined since the early 1960s [1], albeit not as extensively as TiO$_2$ owing to the inherent photocorrosion of ZnO when subjected to UV radiation at wavelengths that activate this semiconductor [2]. With the first report of the photoelectrochemically-assisted splitting of water by UV-irradiated $n$-TiO$_2$ electrodes to H$_2$ and O$_2$ by Fujishima and Honda [3] in the early 1970s, research shifted to using TiO$_2$, also a UV semiconductor that possesses unusually high chemical and photochemical stability and cost is relatively low. Not until the early 1990s did extensive research in using titanium dioxide (in powdered form; e.g. Degussa

P-25 TiO$_2$) take-on its own characteristic speed as a potential environmental photocatalyst, which has led to a technology now commonly referred to as Heterogeneous Photocatalysis [4,5]. Despite the extensive number of studies in this area, however, large-scale treatments of polluted aquatic environments utilizing this technology have been relatively scarce because of some unresolved issues, not least of which are the low efficiencies observed in the photodegradation of a large number of organic polluting substrates.

To enhance these otherwise low efficient processes, we have begun a systematic examination into the photodegradation of some organic pollutants using UV/vis irradiation coupled to microwave radiation [6]. Photodegradations can be enhanced by the microwave radiation even under severe conditions such as small quantities of TiO$_2$ used, low concentration of dissolved oxygen in the aquatic environment and the rather low light irradiance typically available. The specific behavior of the TiO$_2$ surface under irradiation with microwaves has also been assessed [7]. Process efficiencies are indeed significantly enhanced by the microwave radiation whose effects on the TiO$_2$ reaction cannot be interpreted as simply being caused by microwave dielectric

heating (thermal effect; i.e. a caloric effect) – other effects that are non-thermal (i.e. non-caloric) in nature also play a role, albeit often an elusive role [8–10].

The dynamics of the microwave-/photo-assisted degradation of bisphenol A (BPA) in aqueous TiO$_2$ dispersions are dramatically improved under ambient temperature conditions [11], suggesting that the microwave radiation is not a simple heat source. In fact, when the microwave's electromagnetic radiation field interacts with the dielectric materials, in addition to generating heat through dielectric polarization (the thermal factor), it can also increase the contact probability between molecules and atoms of the reacting substrates thereby causing an enhancement of the reaction rates and a lowering of the activation energies (the non-thermal factor) [12]. Other mechanisms such as electric conduction and magnetic field hysteresis loss can also convert the microwave radiation field (electric field, **E**, and magnetic field, **H**) to volumetric heating of a dielectric material through energy losses [13].

In the present study, we examined those special effects that microwaves can impart on the ZnO and TiO$_2$ (P-25) metal oxides from an investigation of the roles of the microwave-generated magnetic (**H**) and electric (**E**) fields. To the best of our knowledge, the effects (or lack thereof) of the microwave radiation on a chemical reaction have thus far not been described in terms of magnetic and/or electric field effects.

## 2. Experimental

### 2.1. Chemical reagents and analytical procedures

High-purity grade 4-chlorophenol (4-CP) was purchased from Tokyo Kasei Kogyo Co. Ltd. Zinc oxide (particle size, 456 nm by TEM microscopy; BET specific surface area, 3.8 m$^2$ g$^{-1}$) and titanium dioxide powdered samples were Wako Pure Chemicals Co. Ltd. and Degussa P-25 grade, respectively.

The time profiles of the disappearance of 4-chlorophenol during the degradation process were obtained using a JASCO high-pressure liquid chromatograph (HPLC) equipped with a JASCO UV-2070 UV/visible diode array multi-wavelength detector and a JASCO Crestpak C-18S column; the eluent was a mixed solution of methanol and H$_2$O (1:1). The number of •OH radicals photo-generated in UV- and microwave-irradiated TiO$_2$ aqueous suspensions was determined relative to a Mn$^{2+}$ standard by EPR spectroscopy using the DMPO (5,5-dimethyl-1-pyrrolidine-N-oxide) spin trap according to a procedure reported earlier [14].

### 2.2. Experimental setup

The continuous microwave irradiation setup with single-mode cavity (TE$_{103}$) is schematically illustrated in Fig. 1. An air-equilibrated aqueous 4-CP solution (0.020 mM; 2.0 mL) containing the metal-oxide particles (loading, 6 mg) was introduced into a quartz sample tube (height, 100 mm; internal diameter, 8 mm) set in the waveguide. The UV irradiation was supplied by an Ushio 250-W Hg lamp (light irradiance, 0.85 mW cm$^{-2}$; wavelength range, 310–400 nm) through the side of the waveguide by a stainless-steel pipe-guide. The temperature of the solution was measured with an infrared thermometer that was previously calibrated with an optical fiber thermometer (FL-2000, Anritsu Meter Co. Ltd.). Temperature fluctuations in the reactor measured with both probes were less than ±2 °C.

The microwave radiation was transmitted to the sample employing an air-cooling isolator, a three-stub tuner, a power monitor and the iris. Avoidance of refluxing the sample was achieved by blowing cold air onto the sample tube. Optimization of low microwave reflection was obtained with an automatic short plunger. The sample tube was located at the maximum density of
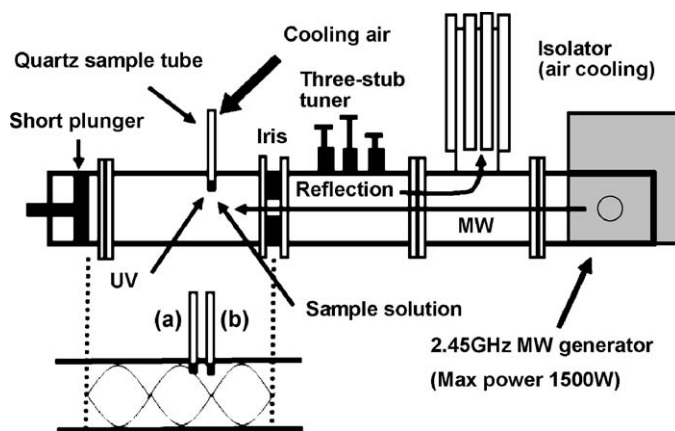


**Fig. 1.** Details of the experimental setup with both UV and microwave irradiation capabilities in the single-mode microwave applicator. Inset (a): sample position in the UV/MW-**EH** method; inset (b): sample position in the UV/MW-**H** method.

the magnetic field (Fig. 1, position (a)) and at the mixture density of the magnetic and electric fields (Fig. 1, position (b)).

The wavelength of the propagation of microwaves in the TE$_{103}$ mode within the waveguide was estimated to be ca. 14.7 cm by the following expression (Eq. (1)) [15], where λ is the wavelength in

$$\lambda = \frac{\lambda_0}{\sqrt{1 - (\lambda_0/2b)^2}} \tag{1}$$

the waveguide; λ$_0$ = 12.24 cm is the wavelength in vacuum given by c/f, {c being the speed of light, 2.9979 × 10$^{10}$ cm s$^{-1}$ and f the microwave frequency 2.45 × 10$^9$ s$^{-1}$}; and b is the length of the waveguide, 10.92 cm.

Unless otherwise noted, the waveguide used was in the TE$_{103}$ mode. The distance of the waveguide between the iris and the short plunger was 1.5 cm. Accordingly, the total internal wavelength of the standing wave was 22.05 cm (14.7 × 1.5 cm). The position of maximum intensity of the magnetic field in the waveguide was 7.35 cm, i.e. at 1/3 the wavelength of the standing wave between the iris and the short plunger (see Fig. 1, position (b)). By contrast, the maximal intensity of the electric field from the iris was at 1/6 the wavelength of the standing wave in the waveguide, namely 3.68 cm. In practice, however, the maximal positions of the intensities of the magnetic field and electric field are shifted slightly by the presence of the sample, a shift that can be compensated for by a simple adjustment of the plunger. This preliminary operation was carried out prior to any further experimentation. We hasten to point out that whenever the **E** or the **H** field was used, we refer to microwave irradiation with a predominantly **E** field or a predominantly **H** field as the two fields cannot be divorced entirely from one another [16]. In other words, although the **E** or **H** field can theoretically irradiate the sample solution at the positions indicated in Fig. 1, with the adjustment necessary to correct for the shift, the sample was being irradiated at the point where the radiation was rich in either the **E** or **H** fields. For these particular experiments, the applied power of the microwave radiation was ca. 20–23 W.

### 2.3. Experimental procedures

Four different methods were used to examine the decomposition of the 4-chlorophenol toxin occurring in the quartz reactor shown in Fig. 1: (i) photocatalytic degradation under concomitant UV light and microwave irradiation with both electric and magnetic fields (UV/MW-**EH** method) in ZnO or TiO$_2$ aqueous
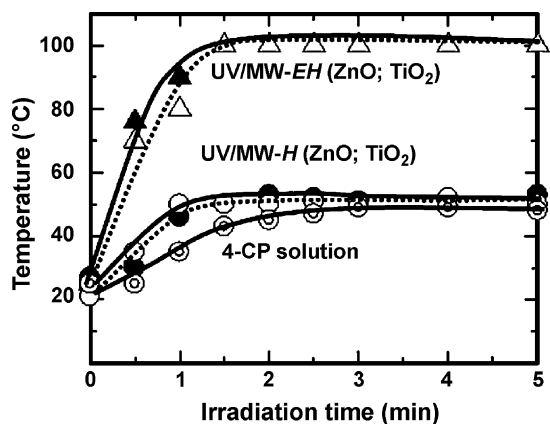
**Fig. 2.** Temperature–time profiles for the various degradation processes occurring in the aqueous dispersions (solid symbols: ZnO; empty symbols: TiO₂) and in a pure 4-CP aqueous solution, also irradiated using the UV/MW-**H** method.

dispersions located in a position of mixed electric and magnetic fields; (ii) the microwave-assisted photodegradation of 4-CP in dispersions with the samples located at a position rich in the magnetic field (UV/MW-**H** method); (iii) photodegradation of 4-CP in the dispersions by UV irradiation alone (UV) under conditions otherwise similar to those above (but no microwaves); and (iv) photodegradation of 4-CP with UV light in dispersions externally heated by conventional methods with an electric heater (UV/CH). The temperature (error less than ca. $\pm 1\,^\circ$C) and pressure were controlled in a manner identical to those used for the UV/MW-**EH** method.

## 3. Results and discussion

### 3.1. Temperature–time profiles

The extent of interaction (i.e. coupling) between the microwave radiation fields (**E** and **H**) and materials, i.e. the efficiency of absorption of the microwaves, is best demonstrated in assessing the temperature–time profiles of the materials during microwave irradiation. In this regard, the profiles of aqueous 4-CP dispersions subjected to the UV/MW-**EH**, UV/MW-**H**, UV/CH and UV procedures are reported in Fig. 2. No temperature differences were observed in the profiles of the TiO₂ and ZnO systems, regardless of whether heat was generated by the **EH** fields or the **H** field alone. With the UV/MW-**EH** method, the temperature of the ZnO and TiO₂ dispersions increased to about 98 $^\circ$C after ca. 90 s of irradiation. By contrast, when applying microwave radiation rich in magnetic field **H** the temperature of the dispersions reached only 50–53 $^\circ$C. The heating efficiency of the dispersions under the magnetic field was slightly enhanced compared to the pure 4-CP solution, at least in the first few min; after 3 min of irradiation the temperature

reached was the same at ca. 50 $^\circ$C. We suspect that the initial faster rise in temperature for the dispersions, in the latter case, was due to a small electric field component in the UV/MW-**H** procedure (see above). Regardless, microwave coupling was significantly greater when both **E** and **H** fields interacted concomitantly with the materials.

### 3.2. Degradation of 4-CP under various methods

The temporal course of the degradation of 4-CP in aqueous ZnO and TiO₂ dispersions with the UV/MW-**EH**, UV/MW-**H**, UV/CH and UV methods was monitored at 279 nm using HPLC techniques. Results are illustrated in Fig. 3. Aqueous solutions of 4-chlorophenol typically display absorption bands at 194, 223 and 279 nm.

In ZnO dispersions, the rates of degradation of 4-CP by the UV/MW-**EH** method ($k_{obs} = 0.22$ min$^{-1}$) and UV/MW-**H** method ($k_{obs} = 0.23$ min$^{-1}$) were somewhat slower relative to the UV method ($k_{obs} = 0.34$ min$^{-1}$) – see Fig. 3a. It is significant to note that the UV/CH method led to an even slower degradation of the toxin by a factor of ca. 20 ($k_{obs} = 0.017$ min$^{-1}$) compared to the UV method alone. Evidently, conventional heating caused a decrease in the photoactivity of ZnO. Even more important are the tenfold slower degradation kinetics for the UV/CH method ($k_{obs} = 0.017$ min$^{-1}$) relative to the UV/MW-**EH** method ($k_{obs} = 0.22$ min$^{-1}$) despite the process occurring under otherwise identical temperature conditions of the bulk solution. The faster degradation of 4-CP was observed whenever the microwaves were rich in magnetic field as compared to the UV and other methods. These results are consistent if the *heat*, whether from conventional or dielectric sources, caused the decrease of the photoactivity of the metal oxide. We also deduce that the UV/MW-**EH** method was superior to the UV/CH procedure because of the presence of a magnetic field in the former (recall the temperatures were identical in the two cases). Thus, the decrease of photoactivity can be controlled by the magnetic field effect, although for ZnO the photoactivity was somehow decreased by the thermal effect of the microwave radiation. A final point is worth noting for the UV/MW-**EH** and the UV/MW-**H** methods regarding the 4-CP/ZnO dispersions. Although the dynamics are identical in both cases, the extent of degradation of the 4-CP was only 50% for the former method and 75% for the UV/MW-**H** method, both reaching a plateau after 20 min of irradiation. We infer that the microwaves **EH** versus **H** fields may additionally cause the nature of intermediates formed to be different. That is, the fields no doubt also impact on the nature of such intermediates and the degradation pathways of the toxin. At the stage of our current studies, the latter were not the objectives of the present study and are discussed no further, although they certainly raise a few questions.

For TiO₂ (P-25) dispersions, the observed first-order rates of degradation of 4-CP decreased in the order UV/MW-**EH** > UV/MW-**H** $\approx$ UV/CH > UV (Fig. 3b). Contrary to the ZnO case, for which the
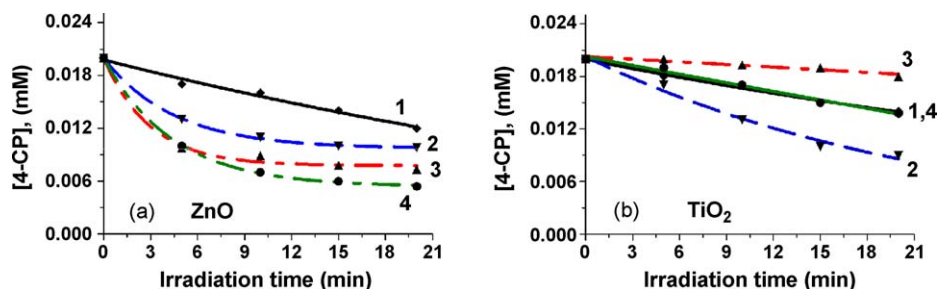


**Fig. 3.** Temporal decrease of 4-CP concentration by using the UV/MW-**EH** (curves 2), UV/MW-**H** (curves 4), UV/CH (curves 1) and UV (curves 3) methods with (a) ZnO (b) TiO₂ (P-25). Estimated errors of each data point are $\pm 5$%.

dynamics of degradation of 4-CP were identical (see above), for TiO$_2$ the UV/MW-**H** method was about 2.6-fold less efficient in degrading the toxin relative to the UV/MW-**EH** method, suggesting an otherwise different effect of the magnetic field on the TiO$_2$ specimen than on ZnO. The observed first-order dynamics for the TiO$_2$ process are $k_{obs}$ = 0.043 min$^{-1}$ (UV/MW-**EH**), 0.020 min$^{-1}$ (UV/MW-**H**), 0.018 min$^{-1}$ (UV/CH) and 0.0052 min$^{-1}$ (UV). We thus infer that there exists a synergistic effect between the electric and magnetic fields that impacts on the photoactivity of TiO$_2$; the total observed first-order rate ($k_{tot}$ = 0.038 min$^{-1}$) of the UV/CH and UV/MW-**H** methods is slightly smaller than the degradation rate observed for the UV/MW-**EH** method ($k_{obs}$ = 0.043 min$^{-1}$).

We infer from the above discussion that the microwave radiation causes different events on the surface and/or in the bulk of the metal-oxide materials, with the root cause likely being the magnetic field. In this regard, a recent examination [17] of microwave specific effects that impact the Raney-Ni and Urushibara-Ni catalysts having different physical and chemical properties, from experiments carried out with conventional and microwave dielectric heating of solutions under otherwise identical temperature conditions, showed that specific effects of the microwaves are not always observed (or occur) in heterogeneous catalysis. More precisely, except perhaps for some cases, catalyzed reactions tend to be influenced mostly by the microwave thermal effect.

In photo-assisted reactions, that are subjected to microwave irradiation conditions, the microwave effect(s) can be ascribed either to a thermal (caloric) or non-thermal (non-caloric) effect or to both. A specific microwave effect has only been seen in a recent study [18] for the P-25 grade of TiO$_2$ particles among other titanium dioxide specimens in which we deduced that P-25 TiO$_2$ must possess some peculiar features that make this specimen behave differently under microwave radiation.

To further elucidate the peculiarity(ies) of P-25 TiO$_2$ relative to ZnO, we examined the number of DMPO–$^•$OH spin adducts (relative to a Mn$^{2+}$ ion standard) that were produced in microwave-irradiated (MW-**EH** alone) and UV-irradiated (UV alone) aqueous dispersions, and for TiO$_2$ and ZnO dispersions simultaneously irradiated with both UV light and microwave radiation (UV/MW-**EH**). The relevant data are reported in Table 1. Note that no $^•$OH radicals were detected in pure aqueous dispersions in the absence of irradiation.

Under microwave irradiation alone (MW-**EH** method), the number of $^•$OH radical formed in the ZnO system was 1.6 times greater than in the TiO$_2$ system, whereas under UV irradiation alone the number of radicals produced was 1.5 times more significant for the ZnO system compared to TiO$_2$. On irradiation with both UV light and microwaves, the number of $^•$OH radicals was 2.2 times greater for ZnO than for TiO$_2$. Comparison of the methods shows that the number of $^•$OH radicals was twofold greater for the UV/MW-**EH** relative to the UV method for the ZnO system. For the TiO$_2$ (P-25) case, it was 1.3 times greater. This was a rather curious result for ZnO. To the extent that a greater number of $^•$OH radicals are produced by the UV/MW-**EH** method, the degradation dynamics of 4-CP were decisively slower than for UV irradiation alone (see Fig. 3a; 0.22 min$^{-1}$ versus 0.34 min$^{-1}$) for

a seemingly twofold greater number of $^•$OH radicals produced. Note that in the $^•$OH radical analysis of Table 1, microwave irradiation (microwave power, 3 W) caused only a small increase of temperature of the solution by ca. 1 °C from ambient. Evidently, the increased temperature in 4-CP/ZnO dispersions in the UV/MW-**EH** method may have caused some changes to this metal-oxide semiconductor. One possibility includes the photocorrosion of ZnO [2] at the higher temperatures (ca. 100 °C; Fig. 2) that we now examine below.

### 3.3. Dielectric properties of ZnO and TiO$_2$ specimens (pellets and powder)

To gain a further understanding of this rather absurd paradox, namely that a greater number of $^•$OH radicals produced by irradiated ZnO should have enhanced the degradation of 4-CP, not inhibit it, we examined the absorption of microwave radiation by ZnO and TiO$_2$ specimens in pellet form; pellets were produced using a press operated under high pressures (ca. 1000 kg cm$^{-2}$) [18]. The dielectric properties of naked pristine ZnO and TiO$_2$ pellets are reported in Table 2; the data for TiO$_2$ (P-25) shown were obtained in an earlier study [17] that examined various TiO$_2$ specimens. The dielectric loss tangent (tan $\delta = \varepsilon''/\varepsilon'$) of the ZnO and TiO$_2$ pellets reflects the *ability* of the material to transform the absorbed microwave's electromagnetic energy into heat, which for ZnO was some 1.6 times greater than for the TiO$_2$ pellet. The greater the loss tangent the more heat is produced, consistent with the results depicted in Fig. 4 (see below). By contrast, the dielectric loss factor ($\varepsilon''$) is a measure of the *efficiency* with which the energy of the electromagnetic energy can be converted into heat [19]. In this case, the ZnO appears slightly more efficient.

Perusal of the data of Table 1 and the results illustrated in Fig. 3 indicates no correlation between the dielectric properties of the two metal oxides and the dynamics of degradation of 4-CP in the aqueous metal-oxide dispersions. The extent of absorption of the

**Table 2**
Dielectric properties at 2.45 GHz for the P-25 TiO$_2$ and ZnO specimens in pellet form[a].

| Specimen | Dielectric loss factor ($\varepsilon''$) | Dielectric constant ($\varepsilon'$) | Dielectric loss tangent (tan $\delta$) |
|---|---|---|---|
| ZnO | 0.189 | 3.430 | 0.0529 |
| TiO$_2$ (P-25) | 0.181 | 5.626 | 0.0322 |

[a] Values of the dielectric properties are those of the TiO$_2$ specimens in pellet form that possibly include trapped air, so that these values may be somewhat different from those of pure TiO$_2$.
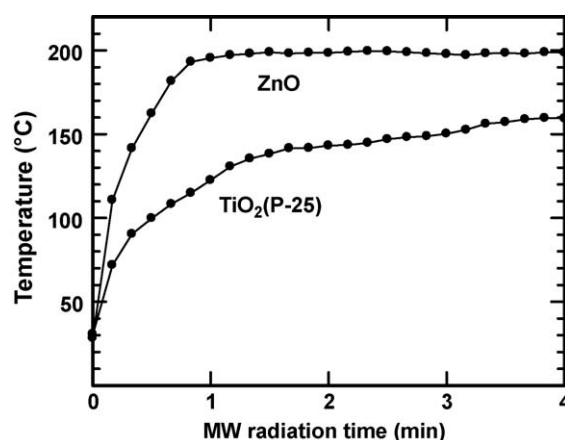


**Fig. 4.** Temperature–time profiles of the absorption of microwave radiation (MW-**EH**) by powdered ZnO and TiO$_2$ specimens packed in a Pyrex tube.

**Table 1**
Relative number of DMPO–$^•$OH spin adducts produced in the ZnO and TiO$_2$ (P-25) heterogeneous systems (no toxin present) under microwave irradiation alone, UV alone and both MW-**EH** and UV irradiations[a].

| | H$_2$O | MW-**EH** | UV | UV/MW-**EH** |
|---|---|---|---|---|
| ZnO | 0 | 1.6 | 11.4 | 22.8 |
| TiO$_2$ (P-25) | 0 | 1 | 7.8 | 10.4 |

[a] Microwave power level, 3 W; change in temperature from ambient was insignificant ($\sim$1 °C).

microwave radiation does not appear to be a factor (either way) in the photoactivity of these metal oxides, since the microwaves are primarily absorbed by the aqueous medium and in a secondary instance by the metal-oxide particles. Evidently the medium attenuates any direct effect of the microwaves on the metal-oxide specimens in this case.

Accordingly, we further examined the level of microwave absorption by the two metal oxides by monitoring the temperature–time profiles (see Fig. 4) of *naked* ZnO and *naked* TiO$_2$ (P-25), this time in powdered form (300 mg) packed in Pyrex tubes. The temperature was measured at the center of the tube/specimen using an appropriately shielded thermocouple. Temperature measurements were performed three times; variations between readings were negligible.

Induction heating of the two metal oxides by the magnetic field **H** of the microwave radiation should be relatively non-existent for the ZnO and TiO$_2$ specimens (however, see below), which show no collective magnetic behavior that would be typical of a ferromagnetic material. Accordingly, any increase in temperature of the two metal-oxide specimens should originate principally from the electric field **E** of the microwaves. The temperature–time profiles displayed in Fig. 4 show that the ZnO powdered specimen reached maximal temperature of ca. 200 °C in less than a minute, whereas the temperature of the TiO$_2$ powdered sample continued to increase even after 4 min of microwave irradiation (ca. 160 °C). The rate of increase of temperature in ZnO was faster. Evidently, the ZnO material is strongly coupled to the microwave radiation fields, whereas the TiO$_2$ moderately so, and as observed by Takizawa et al. [13] the coupling between the MW-**EH** fields and ZnO increases with the rise of temperature. Our results are also in accord with those of Fukushima et al. [20] who investigated the sintering of ZnO and TiO$_2$ (P-25) powders by microwave irradiation.

Both ZnO and TiO$_2$ are n-type semiconductor materials owing to their non-stoichiometric nature, with inherent defect centers (e.g., anion vacancies and F-type color centers, and Ti$^{3+}$ centers in the case of TiO$_2$) at the surface and in the bulk of the particles [21]. Crystalline solids such as non-stoichiometric ZnO (rocksalt, zincblende and wurtzite) and TiO$_2$ (anatase, rutile and brookite) structures have a free energy ($G$) that is always smaller than the free energy of the amorphous phase of analogous composition, so that transformation from a crystalline solid to the amorphous state is energetically not allowed. Yet, irradiation with 2.45-GHz microwaves, predominantly rich in magnetic field, led to extremely rapid heating up to 1000 °C through magnetic induction within a few seconds causing the crystalline solids to be converted to amorphous solids [16]. Stoichiometric TiO$_2$ does not appear to suffer the same fate, unless pre-reduced in a H$_2$ atmosphere or doped with metal cations. Under our experimental conditions, irradiation with 2.45 GHz microwaves (MW-**EH**) is unlikely to cause such decrystallization [22] of either ZnO or TiO$_2$ at the temperatures reached in Fig. 4.

### 3.4. Thermal effect on the degradation of 4-CP in ZnO dispersions

Considering that the greater temperature increase in ZnO might affect the degradation of 4-CP, we next investigated the microwave irradiation (UV/MW-**EH**) of aqueous dispersions containing ZnO and the 4-CP substrate under cooled conditions (UV/MW-**EH**/Cool) so as to minimize, if not suppress, the thermal factor for the process occurring on the ZnO surface in the reactor illustrated in Fig. 5.

The integrated Pyrex microwave-/photo-reactor was equipped with a cooling system comprised of an oil bath and a cooling coil made of microwave non-absorbing material. The microwave radiation source was a Tokyo Rikakikai Co. Ltd. MWO-1000S system consisting of a microwave generator (frequency, 2.45 GHz) and a multimode applicator. The microwave source continuously
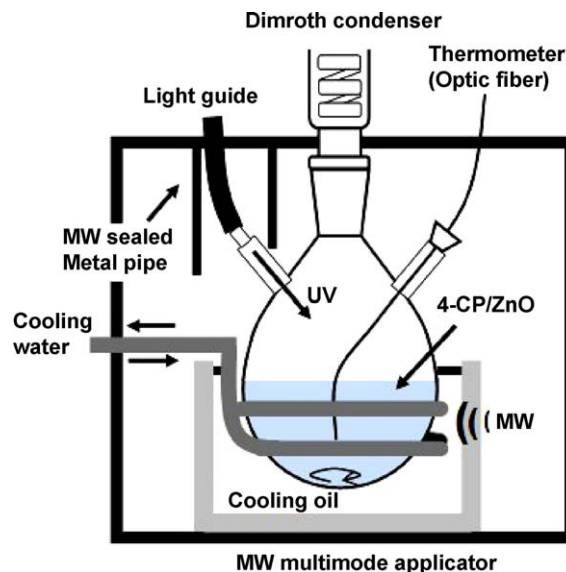


**Fig. 5.** Schematic illustration of the microwave-assisted photoreactor with a cooling system in the microwave multimode applicator. Note that the cooling coil was composed of a microwave non-absorbing material.

irradiated the sample at 100-W power. The reaction temperature was maintained ambient with a Tokyo Rikakikai Co. Ltd. MWO-1000 chemical reaction system for microwave heating and cooling using a circulation system. On the other hand, when using the UV/MW-**EH** method the solution temperature increased to 100 °C under microwave heating (no cooling). The UV light source was a super high-pressure 150-W mercury lamp irradiating the samples from the top of the reactor through a light guide. Other details were described elsewhere [11]. Results of the degradation of 4-CP under these conditions are illustrated in Fig. 6. Note that the (nearly ambient) temperature of the process under UV irradiation alone (ca. 24 °C) was similar to that of the UV/MW-**EH**/Cool method (ca. 27 °C).

The data of Fig. 6 demonstrate an enhancement of the degradation of 4-CP at the lower temperatures with the UV/MW-**EH**/Cool method ($k_{obs} = 0.062 \pm 0.014$ min$^{-1}$) relative to the UV/MW-**EH** methodology ($T \approx 100$ °C after 10 min; $k_{obs} = 0.038 \pm 0.003$ min$^{-1}$) under otherwise identical conditions of microwave power (compare curves 3 and 1). The dynamics for the UV irradiation alone were within experimental error ($k_{obs} = 0.052 \pm 0.008$ min$^{-1}$) identical to the UV/MW-**EH**/Cool method at otherwise similar temperatures (24 °C versus 27 °C; see curves 2 and 3).
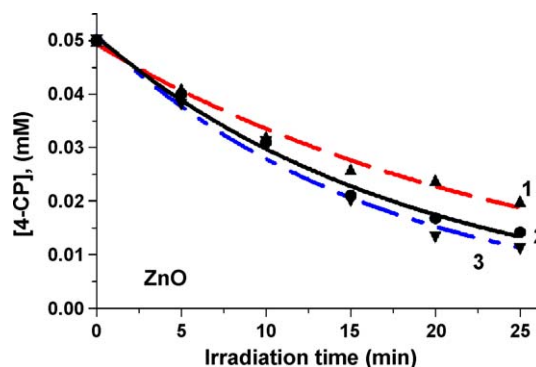


**Fig. 6.** Temporal decrease of the concentration of 4-chlorophenol (0.050 mM) during its decomposition in aqueous ZnO dispersions by the photo-assisted oxidation (UV; curve 2), by the microwave-/photo-assisted oxidation (UV/MW-**EH**; curve 1), and by the integrated microwave-/photo-assisted oxidative method under cooling conditions (UV/MW-**EH**/Cool; curve 3). Note that while curves 2 and 3 are not very different within experimental error, both are different from curve 1.

**Table 3**
Results of the extent of photo-induced corrosion of ZnO under various methods by atomic absorption spectroscopy (100 mg ZnO in 50 mL aqueous media; loading: 2000 mg L$^{-1}$).

| Method | Solution | UV | MW-**EH** [a] | UV/MW-**EH** [a] | UV/MW-**EH**/Cool |
|---|---|---|---|---|---|
| Time (min) | 0 | 30 | 30 | 30 | 30 |
| Zn$^{2+}$ (mg L$^{-1}$) [b] | 0.66 | 1.06 | 0.40 | <0.1 | 0.82 |
| %Corrosion | 0.03 | 0.05 | 0.02 | <0.005 | 0.04 |

[a] Under reflux conditions.
[b] May also include nanoparticles of ZnO that passed through the 0.10 μm filter.

Given the well-known photo-induced corrosion of ZnO to Zn$^{2+}$ ions in aqueous media under UV irradiation [2], the corrosion of ZnO may have been even more pronounced when further irradiated by microwaves whose absorption efficiency was significantly greater compared to TiO$_2$. Accordingly we examined the extent of photo-induced corrosion of ZnO by atomic absorption spectrometry (ICP; Seiko Instruments Inc. Model SAS-7500A) for dispersions containing 100 mg of ZnO in 50 mL ion-exchanged water (pH 6.5; ZnO loading: 2.0 g L$^{-1}$) that were subsequently sonicated for 30 s. After the irradiation treatments noted below, the dispersions were filtered through a 0.10 μm filter just prior to the ICP analyses; the results are summarized in Table 3. It is clear that photocorrosion, if any, was negligible under our experimental conditions.

Thus, the slower dynamics of the photodegradation of 4-CP seen in Fig. 6 in aqueous ZnO dispersions cannot be ascribed to photocorrosion of the ZnO specimen even at the higher temperature of 100 °C for the UV/MW-**EH** method relative to the UV/MW-**EH**/Cool method (ca. 27 °C). Rather, a likely cause of the slower dynamics at the higher temperature may be (a) the possible annealing of trap sites (defect centers) for electrons and holes photogenerated in the UV/MW-irradiated ZnO thereby enhancing electron–hole recombination, and/or (b) thermally-stimulated ionization of trapped charge carriers that would also ultimately enhance such charge carrier recombination. The latter hypotheses will be examined in a subsequent study using time-resolved picosecond laser spectroscopy for both the TiO$_2$ and ZnO semiconductor colloidal specimens under microwave irradiation.

## 4. Concluding remarks

The microwave specific effect(s) on a photo-assisted reaction, such as the photooxidative degradation of chlorinated phenols (e.g. herein, 4-CP), can be imparted by the magnetic field of the microwave radiation. As such, the thermal (caloric) and/or non-thermal (non-caloric) effect(s) of the microwaves on processes and/or on materials (e.g. metal oxides), in principle, can be delineated between the magnetic field and the electric field. In the present instance, the microwave effect(s) on the ZnO and TiO$_2$ materials basically differed in kind. In the case of ZnO, the photoactivity was enhanced by the microwave specific (non-caloric) effect originating in large part from the microwaves'

magnetic field **H**. By contrast, its photoactivity was decreased by the thermal factor originating from the microwaves' electric field **E**. Contrary to ZnO, the photoactivity of TiO$_2$ (P-25) was enhanced by the synergistic effect of both the magnetic and electric fields of the microwave radiation.

## References

[1] M.C. Markham, J.C. Kuriacose, J.A. DeMarco, C. Giaquinto, J. Phys. Chem. 66 (1962) 932.
[2] E. Garcia-Lopez, G. Marci, N. Serpone, H. Hidaka, J. Phys. Chem. C 111 (2007) 18025.
[3] A. Fujishima, K. Honda, Nature 238 (1972) 37.
[4] (a) N. Serpone, E. Pelizzetti (Eds.), Photocatalysis—Fundamentals and Applications, Wiley, New York, 1989;
(b) M.R. Hoffmann, S.T. Martin, W. Choi, D.W. Bahnemann, Chem. Rev. 95 (1995) 69.
[5] A. Fujishima, K. Hashimoto, T. Watanabe, TiO$_2$ Photocatalysis—Fundamentals and Applications, BKC, Tokyo, 1999.
[6] S. Horikoshi, N. Serpone, H. Hidaka, Proc. 7th Intern. Conf. on TiO$_2$ Photocatalytic Purification Treatment of Water and Air, London, ON, Canada, (2000), p. 102.
[7] S. Horikoshi, H. Hidaka, N. Serpone, Environ. Sci. Technol. 36 (2002) 1357.
[8] S. Horikoshi, A. Saitou, H. Hidaka, N. Serpone, Environ. Sci. Technol. 37 (2003) 5813.
[9] S. Horikoshi, N. Serpone, H. Hidaka, Environ. Sci. Technol. 36 (2002) 5229.
[10] S. Horikoshi, M. Kajitani, H. Hidaka, N. Serpone, J. Photochem. Photobiol. A: Chem. 196 (2008) 159.
[11] S. Horikoshi, M. Kajitani, N. Serpone, J. Photochem. Photobiol. A: Chem. 188 (2007) 1.
[12] C. Shibata, T. Kashima, K. Ohuchi, Jpn. J. Appl. Phys. 35 (1996) 316.
[13] H. Takizawa, M. Iwasaki, T. Kimura, A. Fujiwara, N. Haze, T. Endo, Trans. Mater. Soc. Jpn. 27 (2002) 51.
[14] S. Horikoshi, H. Hidaka, N. Serpone, Chem. Phys. Lett. 376 (2003) 475.
[15] N.J. Cronin, Microwave and Optical Waveguides, Institute of Physics Publishing, Great Britain, 1995, pp. 27–40.
[16] R. Roy, Y. Fang, J. Cheng, D.K. Agrawal, J. Am. Ceram. Soc. 83 (2005) 1640.
[17] S. Horikoshi, J. Tsuzuki, F. Sakai, M. Kajitani, N. Serpone, Chem. Commun. (2008) 4501.
[18] S. Horikoshi, F. Sakai, M. Kajitani, M. Abe, A.V. Emeline, N. Serpone, J. Phys. Chem. C 113 (2009) 5649.
[19] D.M.P. Mingos, D.R. Baghurst, Chem. Soc. Rev. 20 (1991) 1.
[20] H. Fukushima, G. Watanabe, H. Mori, M. Matsui, Toyota R&D Rev. (Japan) 30 (1995) 25.
[21] (a) See for example: V.N. Kuznetsov, N. Serpone, J. Phys. Chem. C, 113 (2009), doi:10.1021/jp901024t; http://pubs.acs.org|doi:10.1021/jp901034t;
(b) A.V. Emeline, V.N. Kuznetsov, V.K. Ryabchuk, N. Serpone, Intern. J. Photoenergy (2008), doi:10.1155/2008/258394;
(c) V.N. Kuznetsov, N. Serpone, J. Phys. Chem. C 111 (2007) 15277;
(d) V.N. Kuznetsov, N. Serpone, J. Phys. Chem. B 110 (2006) 25203;
(e) N. Serpone, J. Phys. Chem. B 110 (2006) 24287.
[22] R. Roy, R. Peelamedu, L. Hurtt, J. Cheng, D. Agrawal, Mater. Res. Innovat. 6 (2002) 128.